International Journal of Geo-Energy

Int. J. Geo-Energy 2023.1(1)
ISSN: 2958-2857
https://doi.org/10.58531/ijge10310001

Article

Study on Denoising Microseismic Signal Based on Autoencoder Convolutional Neural Networks

Shibin Tang [1,*], Fusheng Liu [2], Chun Zhu [3], Ximao Chen [4], Xingzhao Wang [5], Zhengzheng Wang [1], Leyu Chao [1], Yan Su [2], Li Zhao [2], Jiaming Li [1], Shun Ding [1], Muhuo Lai [6]

[1] School of Civil Engineering, Dalian University of Technology, Dalian, 116024, China

[2] Hanjiang-to-Weihe River Valley Water Diversion Project Construction Co., Ltd., Xi'an, 710010, China

[3] School of Earth Sciences and Engineering, Hohai University, Nanjing, 210098, China

[4] Fujian Railway Construction Co., Ltd. of China Railway 24th Bureau Group, Fuzhou, 350013, China

[5] China Railway 24th Bureau Group, Fuzhou, 350013, China

[6] China Construction Fourth Engineering Division Co. Ltd., Guangzhou, 511400, China

*Correspondence: Shibin Tang, tang_shibin@dlut.edu.cn

Academic Editor: Dr. Sela Akdag <s.akdag@unsw.edu.au>

Received: 8 December 2022; Revised: 18 December 2022; Accepted: 25 December 2022; Published: 1 January 2023

Abstract: As a kind of dynamic real-time monitoring technology, microseismic monitoring technology has been widely used for rockburst warning. Due to the complexity of the actual monitoring environment, the monitoring signals often contain different types of noise, affecting the earning warning of rockburst. In this study, an Autoencoder Convolutional Neural Network denoising model based on deep learning has been proposed to denoising of the complex signals. The unsupervised adaptive training method is used to train the model, which only needs to set its initial parameters. The importance of an enhanced training dataset is illustrated by the comparison experiment. The results indicate that the training and verification shows well performance during training. The denoising efficiency of the proposed model is studied by the denoising of the synthetic noise-containing signals. Furthermore, the dataset from the water conveyance tunnel in the Hanjiang-to-Weihe River water diversion project (HJ-Project) in Shaanxi Province is taken as an engineering example to evolute the performance of the proposed model for practical project. The denoising performance of the model is analysed through the visual denoising results and evaluation index. The model can effectively denoise the complex noised signal which separate it into pure microseismic

Citation: Tang S, Liu F, Zhu C, Chen X, Wang X, Wang Z, Chao L, Su Y, Zhao L, Li J, Ding S, Lai M. Study on Denoising Microseismic Signal Based on Autoencoder Convolutional Neural Networks. Int. J. Geo-Energy, 2023, 1(1), doi: 10.58531/ijge10310001

signal and noise signal, and improve the signal-to-noise ratio, which is benefit for arrive-time picking and source locating then improve the performance of early warning of rockburst.

Keywords: microseismic monitoring; rockburst; deep learning; denoising; convolutional neural network

1. Introduction

Due to the uneven spatial distribution of water resources and serious water shortage in local areas, China has carried out large-scale water conservancy projects. With the development of the construction of water conservancy project, many rock mechanics problems have also been brought in the process of project construction, especially the problem of serious rockburst, which poses a security threat to construction personnel and mechanical equipment [1,2]. In recent years, the use of microseismic monitoring technology for early warning of rock burst hazards is the most popular technique. However, due to the complexity of the actual environment of construction of rock engineering project, the quality of the microseismic monitoring signal is serious affect by the many types of noise, and even the noise submerges the microseismic information. This increases the difficulty of signal processing, leading to inaccurate signal identification, difficulty in picking up of the arrival-time, great error of source location and inaccurate hazard warning [3-5]. Therefore, it is necessary to denoise the noisy microseismic signals during the microseismic monitoring.

There are many denoising methods including Fourier Transform (FFT) [6], Short Time Fourier Transform [7], Wavelet Transform (WT) [8,9] and Empirical Mode Decomposition (EMD) [10,11], etc. There are still some problems when these denoising methods are applied to the microseismic signals. Large amount of microseismic data result in the large number of iterations of the algorithm with high complexity of signal, which are prone to redundancy. The partial analysis of the signal is inaccurate, the quality of signal is distorted after denoising, and the signal features and amplitude change strongly, resulting in changes of the original features of the microseismic event signal. Furthermore, these denoising methods have poor engineering adaptability, and the noise cannot be effectively denoised in the face of different types of noisy environment.

The traditional feature extraction algorithm depends on the prior knowledge of data information and the experience of technicians. With the continuous upgrading of task difficulty, it cannot achieve ideal results which shows poor adaptability. With the continuous improvement of hardware performance and software algorithms, deep learning [12] as a powerful artificial intelligence algorithm, has been widely used in computer vision, engineering data mining, text classification and other fields, which has achieved better results than traditional methods. Deep learning uses a large amount of data to train the characteristics of model learning objectives by building a deep nonlinear network, and uses the trained model to complete the mapping of task objectives [13-15]. There are many proposed methods of denoising by deep learning. Li et al. [16] proposed a fast and flexible convolutional neural network (FFCNN), which introduces transfer learning into the data training process to achieve seismic data denoising. Guo et al. [17] proposed a new end to end mapping trainable microseismic data reconstruction network model, which can effectively denoise of microseismic signal. Zhang et al. [18] proposed a neural network model combining convolutional neural network (CNN) and short-term and long-term memory (LSTM), which uses edge components for event detection and denoising training, and is suitable for denoising of complex signals in mine microseismic monitoring. Zhu et al. [19] proposed a denoising method based on deep convolution neural network, which can learn the sparse representation of time-frequency data, as well as the nonlinear function mapped to the mask, and effectively remove the Gaussian white noise in the coal microseismic signal. It can be seen that those methods show it is effectively of denoising by using the convolutional neural network to denoise the microseismic signals. However, microseismic signals in different projects are also affected by geological factors such as surrounding rock classification and faults, and their waveform characteristics such as frequency and amplitude are different. There is little study on the depth learning method for denoising of microseismic signals in the surrounding rock of deep buried tunnels. Due to deep learning can well learn the characteristics and sparsity of microseismic signals, it is possible to remove the noise signal from microseismic signal to get relatively pure microseismic data. Therefore, it is of great important to study on the microseismic signals denoising based on deep learning.

In this study, a convolutional neural network model is proposed which based on the deep learning method of artificial intelligence, to denoise the microseismic signals. At first, a denoising model of

microseismic signal with noise is proposed by using deep self-coding convolutional neural network. Then, the denoising algorithm of microseismic data is realized by optimizing the training of the convolution neural network. This model can effectively separate noised signal into microseismic signals and noise signal. After denoising, the signal-to-noise ratio (SNR) is significantly improved, and the characteristics of microseismic signals are also well preserved, with strong denoising effect.

2. Engineering background and microseismic monitoring system

Provide sufficient details to allow the work to be reproduced by an independent researcher. Methods that are already published should be summarized, and indicated by a reference. If quoting directly from a previously published method, use quotation marks and also cite the source. Any modifications to existing methods should also be described.

2.1 Engineering background

The Hanjiang-to-Weihe River Diversion Project (HW-Project) is a sub-project of the South-North Water Diversion Project, which is used to meet the water transfer and distribution projects in Xi'an, Xianyang and industrial parks in China. The HW-Project passes through the Yellow River and Yangtze River basins and crosses the Qinling Mountains along the way. The elevation range is about 1050 to 2420 m, and the maximum burial depth of the tunnel is about 2000m. Within the area are mainly quartzite, granite, amphibolite and fault fractured rocks. Stratigraphic overview of the main tunnel area of the water conveyance tunnel is shown in Figure 1. Two faults are present in the project area, i.e., f_7 fault (N80°-85°W/70°-85°N (5°-10°∠70°-85°)) and QF_4 fault (N60°-70°W/70°-80°S (200°~210°∠70°~80°)). The fault zone is mainly filled with fractured rocks, diorite and mylonites.

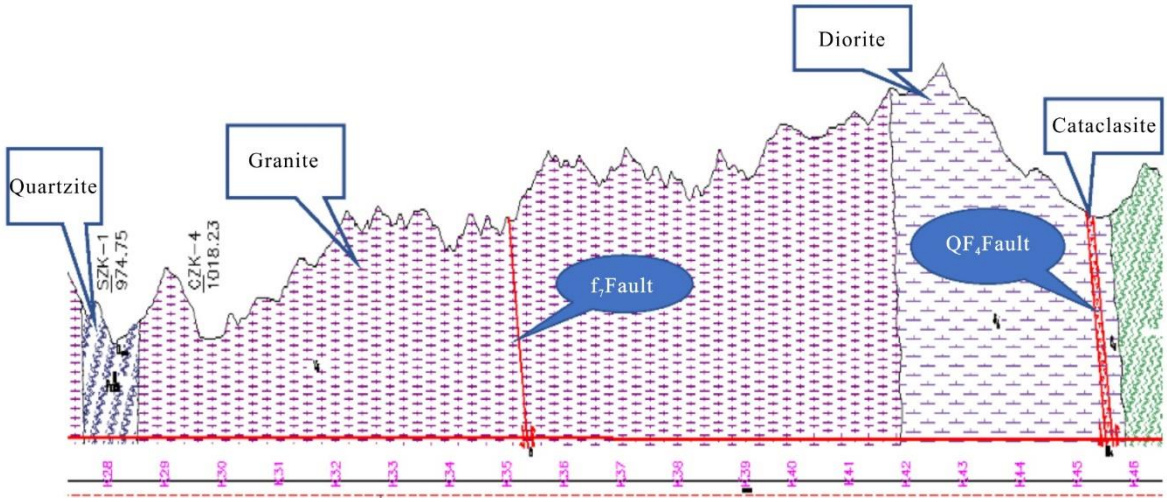

Figure 1 Stratigraphic overview of the main tunnel area of the water conveyance tunnel

2.2 Microseismic monitoring system

The microseismic monitoring system is adopted in the HW-Project to detect the rockburst [20-21]. Mobile microseismic monitoring equipment was built near the TBM working face to realize real-time acquisition, spectrum analysis and 3D visualization of microseismic signals. Composition diagram of microseismic monitoring system is shown in Figure 2. It is mainly divided into three parts: sensor array (the project is equipped with 6 sensors), microseismic signal acquisition system, and upper computer. The accelerometer receives the elastic wave and converts it into an electrical signal. The Paladin data acquisition instrument converts the electrical signal into a digital signal, which is finally transmitted to the Hyperion microseismic signal processing system via optical fiber. When the monitored signal event is higher than the lower threshold set by the system, the Hyperion signal processing system will record the complete waveform information of the signal and visualize it in 3D by SeisVis software at the computer terminal. The processed microseismic event details are automatically saved in the Access Database for later extraction applications.

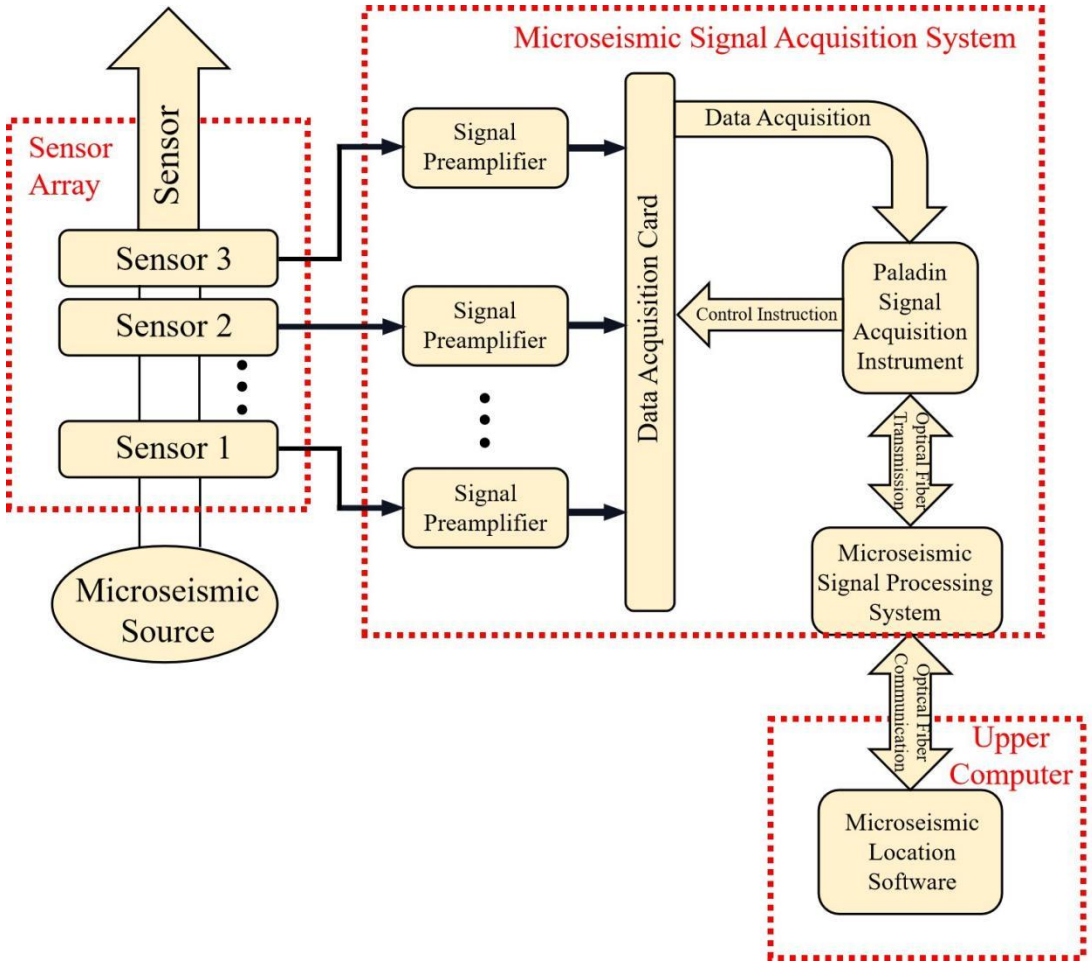

Figure 2 Composition diagram of ESG microseismic monitoring system

In the process of classifying the large number of signal waveforms monitored at the site of the HW-Project, it was found that most of the microseismic signals contained different levels and types of noise. We basically classify the noised microseismic signals into three categories: microseismic signal with construction noise (MS-CN), microseismic signal with current interference (MS-CI), and microseismic signals with both construction noise and current interference (MS-CN-CI), as shown in Figure 3. Fast Fourier Transform (FFT) is a digital conversion technique that converts time domain analysis into frequency domain analysis. By comparing different signal frequency domain features to identify various types of signal frequency characteristics, the accurate identification of microseismic event waveforms lays the foundation for the next step of microseismic signal denoising. The FFT formula [22] is:

$$X(k) = \sum_{n=0}^{N-1} x(n)(cos\ 2\pi k \frac{n}{N} - j\ sin\ 2\pi k \frac{n}{N}) \quad (1)$$

where $x(n)$ represents the time series of signals; $X(k)$ represents the frequency sequence of

microseismic waveform.

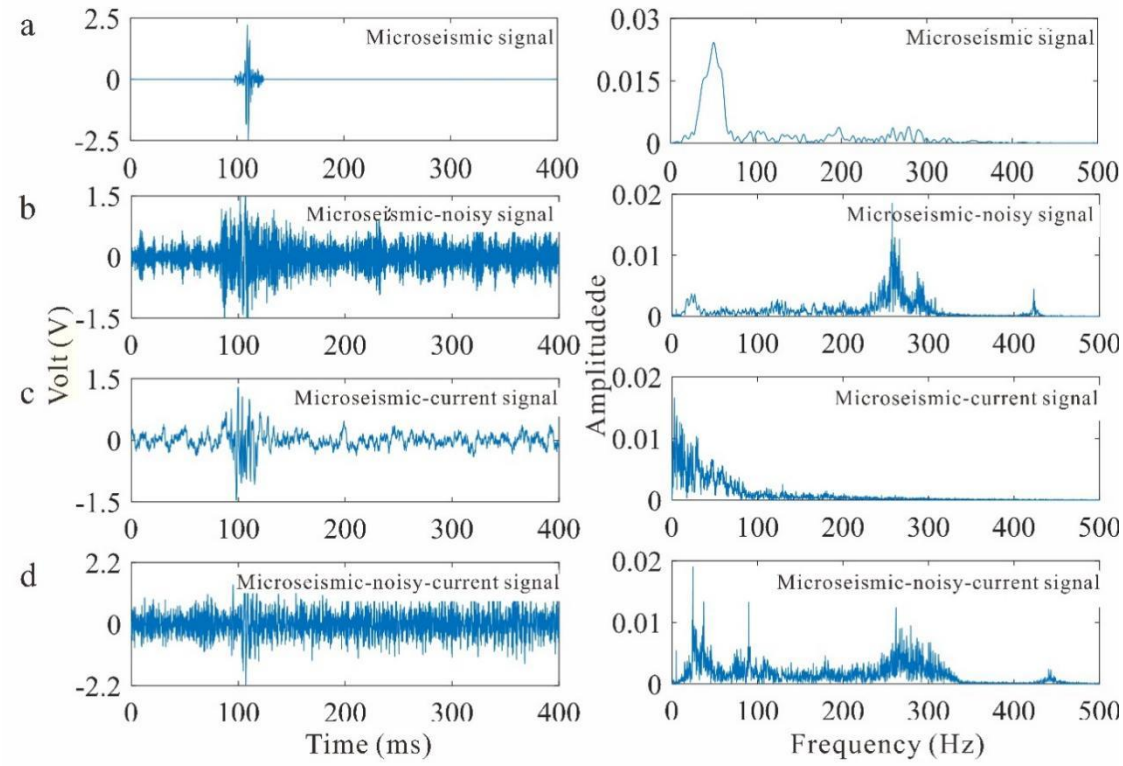

Figure 3 Several typical microseismic signals, (a) pure microseismic signal, (b) signals with construction noise (MS-CN), (c) signals with current interference (MS-CI), (d) signals with both construction noise and current interference (MS-CN-CI).

3. Autoencoder convolutional neural network model

3.1 Autoencoder principle

Autoencoder consists of two main parts: encode and decode [23-24]. The encoder maps the input signal to the feature space which means mapping to the hidden layer：

$$\hat{x} = f(Wx + b) \tag{2}$$

where *x* represents the input signal, $\hat{x}$ represents the hidden layer, f represents the nonlinear function. The function of the decode is to restore the hidden variables of the hidden layer to the initial dimension：

$$y = f(W'x + b') \tag{3}$$

where *y* represents the decoded output, which is the actual network output and the predicted value for the input layer.

Autoencoder is an unsupervised learning model, which learns the features of the input data and reconstructs its structure to compress the input. It is a neural network in which the target output is

equal to the input by back-propagation algorithm. The feature space of the input data is compressed by the encoder, and then the compressed feature is reconstructed and output by the decoder [25]. As shown in Figure 4, The input of the Autoencoder is data *x* without any prior and without difference. The encoder learns feature *Z* from the input data through multi-layer hidden network such as convolution layers and pooling layers, and maps *x* to *Z*. The dimension of *Z* is usually smaller than that of *x*. The main purpose is for dimensionality reduction so as to capture the features of meaningful changing factors in the data and improve the training speed of the model. The Autoencoder is trained by minimizing reconstruction error, which is a measure of the difference between the original input *x* and the reconstructed output *y*. The encoder and decoder output data information by compression and reconstruction of the input data, and optimize and adjust the input and output information by loss function, and finally meet the minimum value of the loss function. This feature of Autoencoder has the function of data dimensionality reduction and compression. When the number of one neuron is greater than that of the next layer of neurons, it can be considered that Autoencoder reduces the dimension of the input data; otherwise, it can be considered that Autoencoder maps the input to a higher dimension [26].

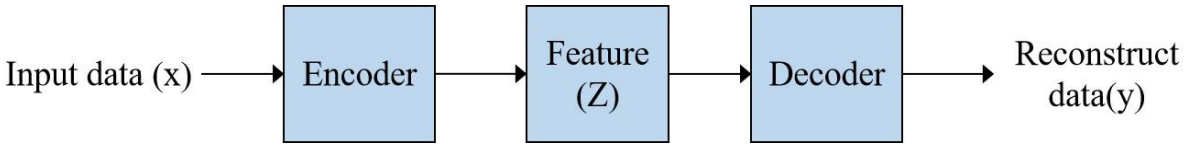

Figure 4 Autoencoder structure

3.2 Building a Network Model

3.2.1 Building the Autoencoder Convolutional Neural Network

All networks in this study were implemented using the MATLAB framework, and it took us about six months to build the Autoencoder Convolutional Neural Network structures. In the structure of Autoencoder Convolutional Neural Network (AECNN) [27-28], the encoder is composed of two convolutional layers and two pooling layers, as shown in Figure 5. The first layer consists of Conv1 and ReLU. Conv1 adopted 64 convolution cores with the size of 3×3 for feature extraction. Pooling1 adopts Max-Pooling operation with the parameter of 2×2 and the step size of 1, and compressed the features identified by the convolution layer to prevent overfitting of convolution operation information.

In the second layer, Conv2 adopts 32 convolution cores with the size of 3×3, and Pooling2 adopts the maximum pooling operation with the parameter of 2×2 and the step size of 1. The decoder consists of two deconvolution layers and two de-pooling layers. The parameter of Deconv1 is 2×2×64 and the ReLU activation function is used. The parameters of Depooling1 is 2×2 and the step size is 1. The deconvolution layer and de-pooling layer are set to map the corner features and main features of microseismic signals extracted by the encoder to recover certain dimensional features. The parameters of Deconv2 is 2×2×32 and the ReLU activation function is used. The parameters of Depooling2 is 2×2 with a step size of 1. Deconv2 and Depooling2 are set up to conduct new mapping of the feature information extracted from the coding so that the resulting feature map, i.e., the denoised microseismic information, corresponded one-to-one with the waveform position of the original image.

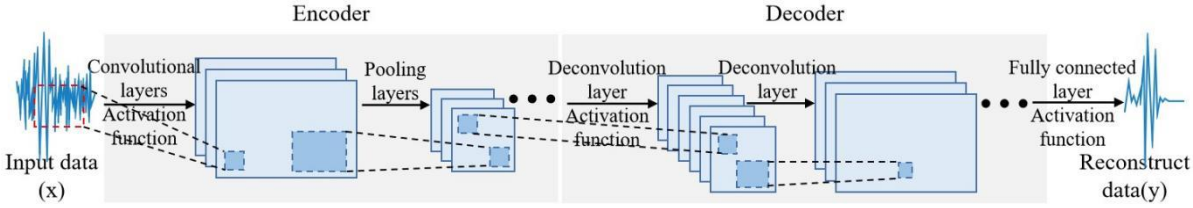

Figure 5 The overall structure of the Autoencoding Convolutional Neural Network

3.2.2 Model training

The training flow chart of AECNN model is shown in Figure 6.

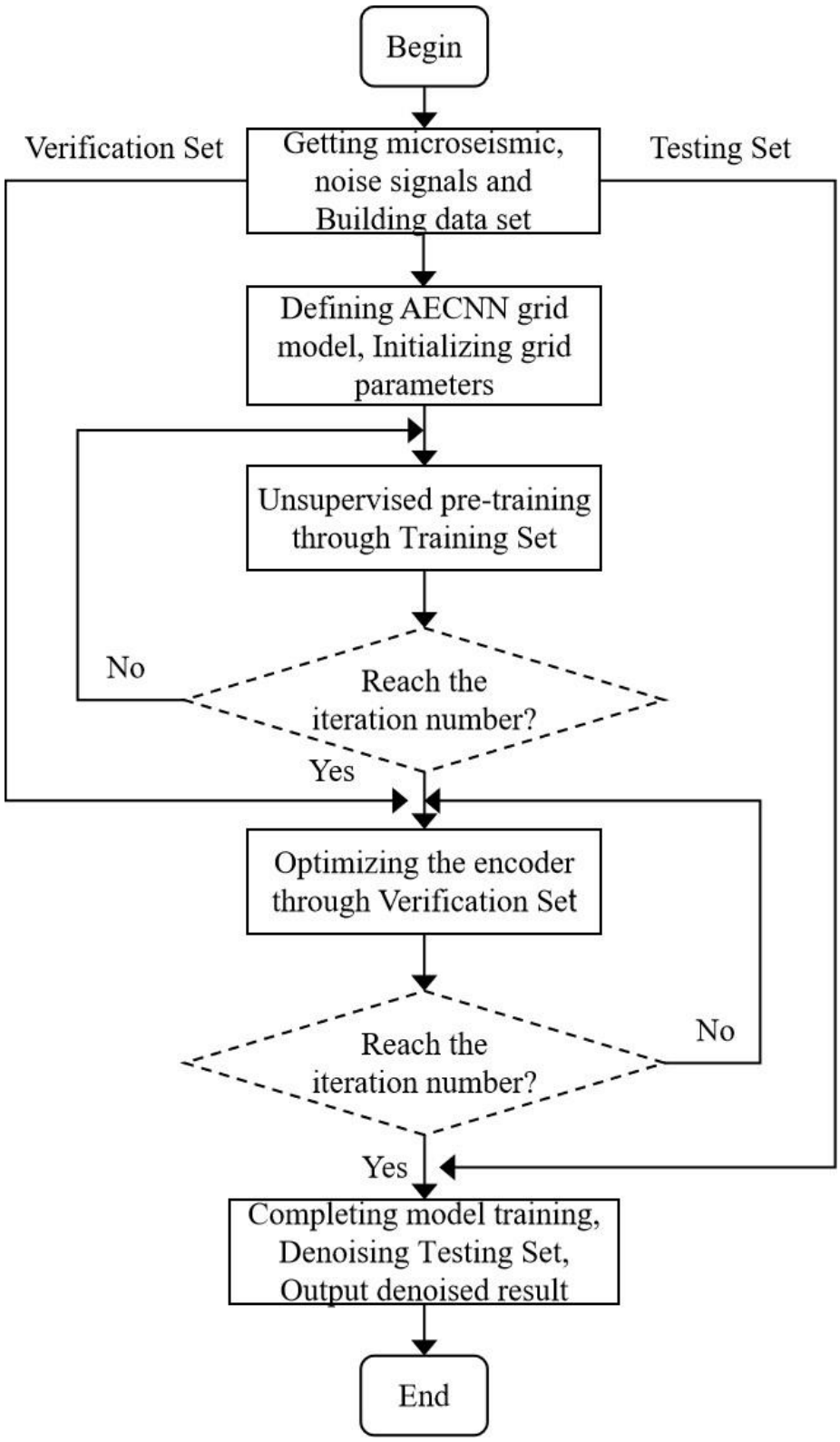

Figure 6 Training flow chart of AECNN model

To build a data set for training, we collect data from the HW-Project. The training data set includes pure microseismic signals (MS), signal of noise (MS-CN, MS-CI and MS-CN-CI). A part of the untrained noisy signals is taken as the validation data set. The noise signal synthesized by MATLAB was used as the test set.

AECNN unsupervised pre-training process: parameters of the convolutional neural network structure layer are set according to the network model construction. The learning rate of adaptive moment estimation (Adam) [29] was set to 0.001 for network optimization. There are no standard rules for setting network parameter values. The parameter values are set according to the experience of previous model training. The AECNN signal denoising model constructed in this paper belongs to the form of adaptive adjustment parameters. Therefore, you only need to set the initial parameters.

Set the number of training iterations for the training sample [30]. Iteration is the act of repeating feedback. In a neural network, only repeated iterative training can achieve the desired goal or result. In general, one iteration equals one training with multiple samples, and the results will be used as the initial value for the next iteration. In this article, the relevant iteration parameter is set to the batch size (batch_size) of 128, the number of iterations (iteration) is 100, set the number of data generation batches to 1000. Make 100 iterations of the training complete 1000 turns, the generalization ability of the model is improved. With the increase of the number of iteration training, the denoising effect tends to be stable. AECNN network model is trained based on Tensorflow 2.6 platform, complete the training and testing of the self-coding convolutional deep neural network on RTX3090GPU. The parallel operation of GPU can greatly improve the computing efficiency of gradient and accelerate the training process of deep neural network.

4 Experimental results and analysis

4.1 Analysis of training and Verification results

Microseismic data sets are a necessary condition for training convolutional neural networks [31-32]. Selecting appropriate sample data can make the model learn, evaluate and analyze abstract features of microseismic data efficiently. The performance of the denoising of the model and sample size play a key role. Since there is no open training dataset applied to microseismic data processing at present, it is necessary to establish a microseismic data set suitable for the denoising training in this paper. In this

paper, a variety of data are used to build data sets. In order to make greater use of the monitored signal data, the monitored signals are classified into pure microseismic, construction noise, current interference, noised microseismic and other types of data.

Due to the huge cost of classification of signal collected by microseismic monitoring, the microseismic data acquired is limited. In order to effectively solve this problem, the data set is enhanced to obtain more training samples and improve the generalization ability of the model. Data enhancement technology is used to expand the data set by mirroring the data, constructing Gaussian white noise, current noise and other methods to make up for the problem of under-fitting caused by insufficient data [33].

In this study, more than 8000 randomly combined microseismic data samples are divided into two parts, 80% of which is used as training data set, 20% as verification data set, and noise signals synthesized by MATLAB are used as test data set.

In order to verify the AECNN model trained by the enhanced training set has a better denoising effect on the signals with noise, the original training dataset and the extended training set were used to train the AECNN model respectively, and two AECNN denoising models with different degrees were generated. The two models were tested by using the noise synthesis signal to observe the denoising effect of the signal.

As can be seen from the denoising effect in Figure 7, there are still a lot of random noises in the signal after the original training set is used to train the AECNN model, which makes it difficult to distinguish microseismic information. Using the enhanced training set to train AECNN model, the random noise in the signal after denoising is eliminated, and the microseismic signal information can be clearly displayed. It is proved that the enhanced training set is better than the original training set to train the AECNN model, and the importance of the enhanced data set in this paper is also verified.

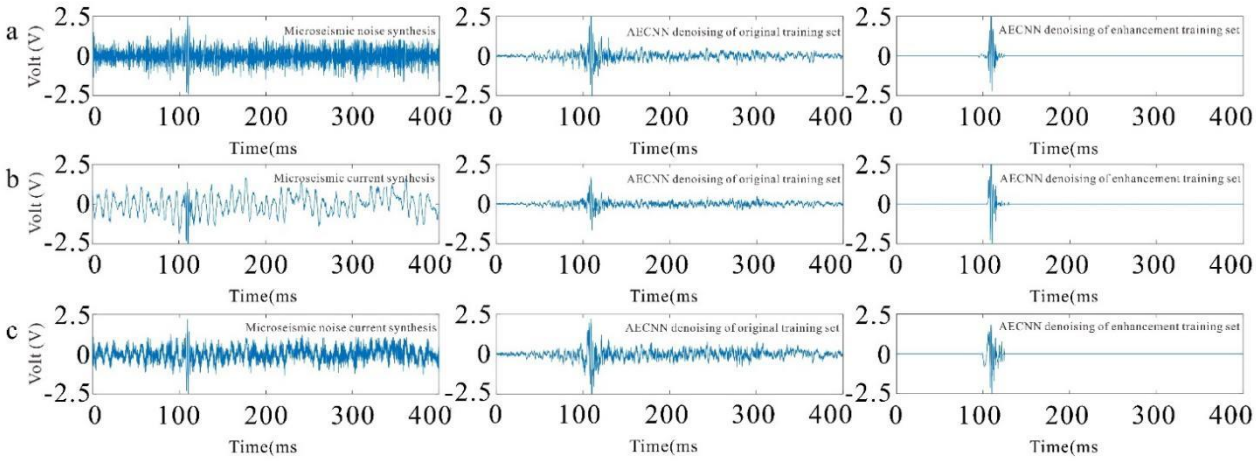

Figure 7 Comparison before and after denoising in the enhanced training set

The changes of accuracy and loss of training and verification datasets are shown in Figure 8. The training accuracy refers to the probability of accurately detecting the microseismic shape of the training set, while the validation accuracy refers to the probability of accurately detecting the microseismic shape of the verification set. Loss represents the learning effect of AECNN model. The smaller the loss value represent the better of the training. After 100 epochs of model training are completed, it is found that in the last 10 epochs, the accuracy rate does not significantly improve and the Loss does not further decrease, and both tend to be stable, which indicates that the training of the model has reached a certain degree of fitting. The accuracy of the final training set and verification set was 97.7% and 95.2%, respectively, while the Loss was 0.0011 and 0.0016. It can be seen that AECNN model performs well in training.

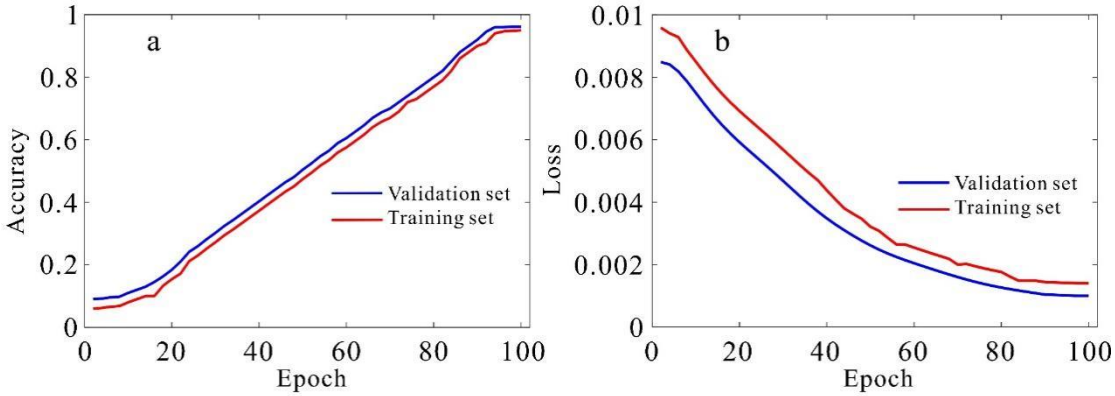

Figure 8 Changes in accuracy and loss during training.

4.2 Denoising experiment of AECNN network model

To test the denoising performance of the model in the time domain, three typical noised microseismic signals, namely signal with noise, signal with current and signal with noise and current, synthesized by the test set MATLAB, are used for denoising test.

AECNN network model is to complete the denoising task of noised microseismic signals, so the final performance of the model is analyzed through visual denoising results. First, the denoising performance of the model is evaluated, including the evaluation of noised microseismic signals and pure noisy signals. In Figures. 9-11, each figure has three columns. The left column shows the noised microseismic signals with different SNR, the middle column shows the signal after overall denoising, and the right column shows the local denoised signal. The noised microseismic signal includes construction noise with different intensity, current interference and mixed noise. The results show that the denoising model can successfully decompose the noise signals with different types and intensities into denoising signals and noises. In addition, the denoised signal loss is very small, and the shape and amplitude characteristics of the denoised signal are well preserved. AECNN has well denoising performance for microseismic signals with various type of noises. In addition, the SNR is greatly improved after denoising, and the denoising effect is superior.

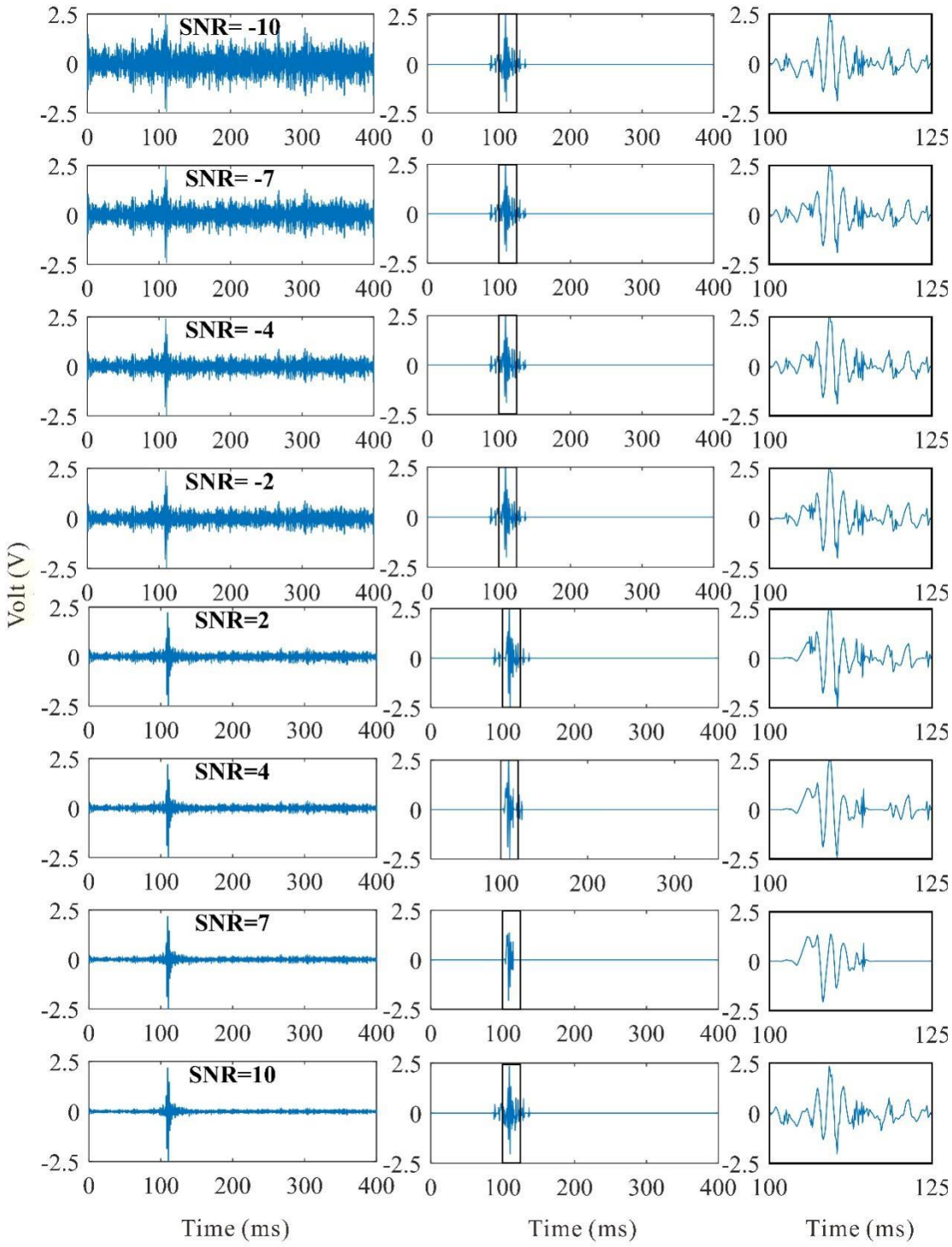

(a) (b) (c)

Figure 9 Denoising efficiency of AECNN model for MS-CN, (a) signal with different SNR, (b) denoised signals and (c) Local denoised results

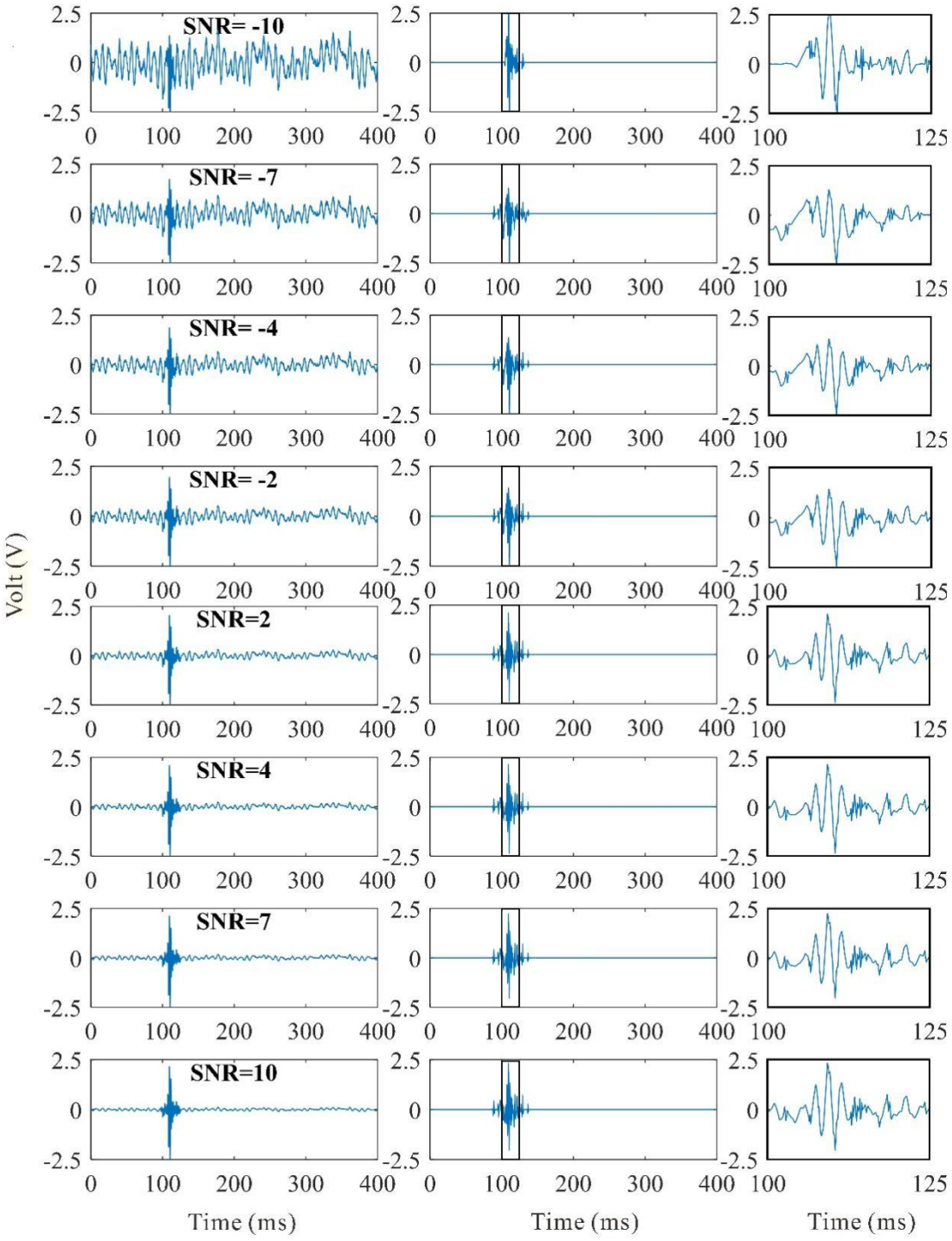

Figure 10 Denoising efficiency of AECNN model for MS-CI, (a) signal with different SNR, (b) denoised signals and (c) Local denoised results

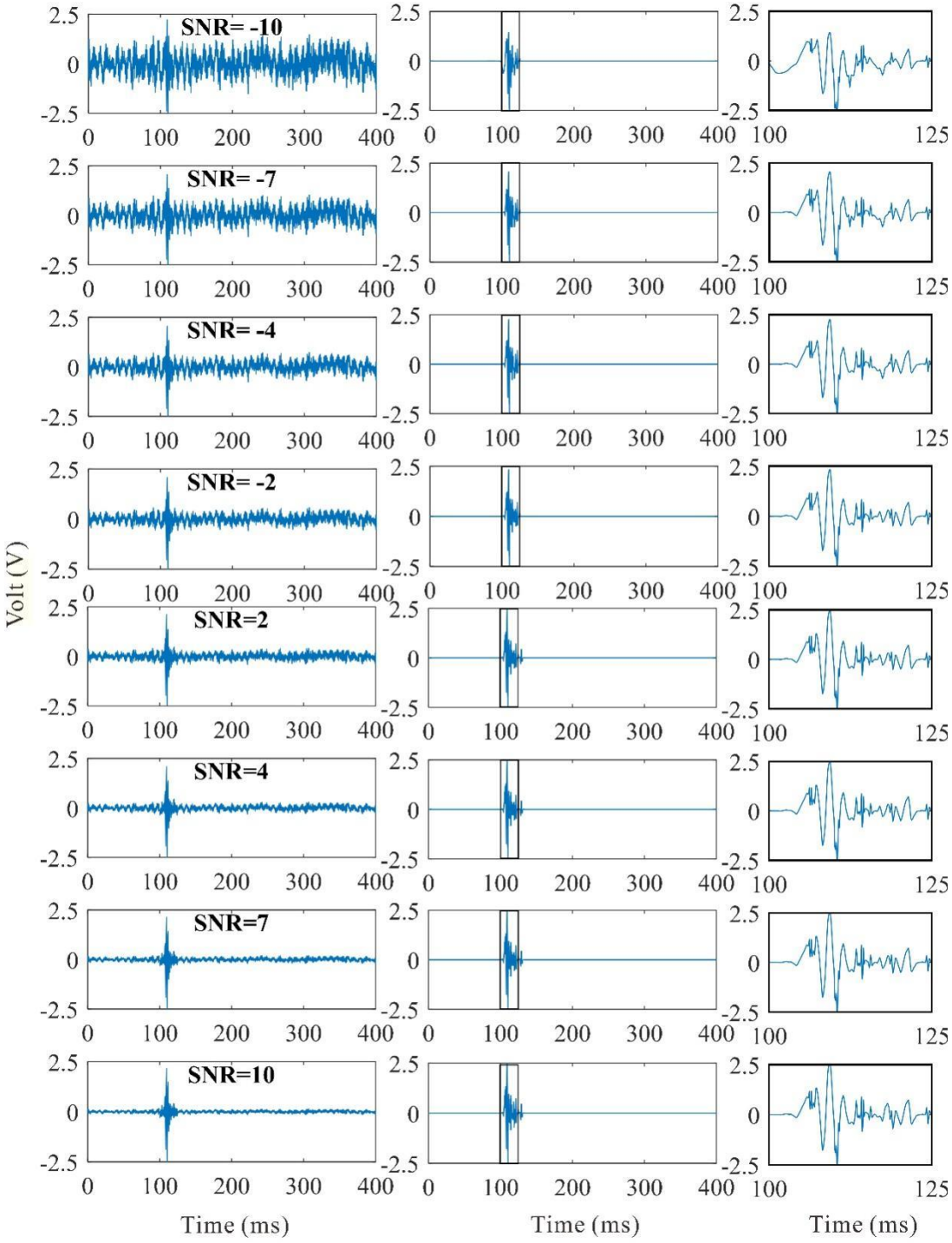

(a) (b) (c)

Figure 11 Denoising efficiency of AECNN model for MS-CN-CI, (a) signal with different SNR, (b) denoised signals and (c) Local denoised results

More importantly, AECNN is also used to conduct noise reduction test on noise samples. Fig. 12 shows the noise reduction effect of AECNN on different types of noise, including construction noise, current interference and noise current mixed noise.

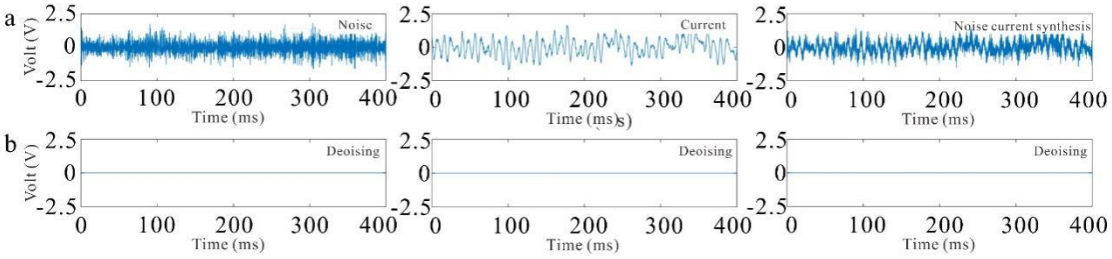

Figure 12 AECNN denoising results for different type of signals (a) the noise signal, (b) the denoising results

The results show the robustness of the denoising to some noisy signals present in the data, that is, the signal after denoising is almost equal to the input data. Fig. 13 shows the distribution of the maximum amplitude difference between the pure noised signal and the denoising results. The results show that the maximum amplitude difference between original and denoised signals is smaller than 0.005V for 60% of noised signals, in which more than 95% signal lose smaller than 0.03V, which indicate that the proposed method is very suitable for the denoising of the noised microseismic signal.

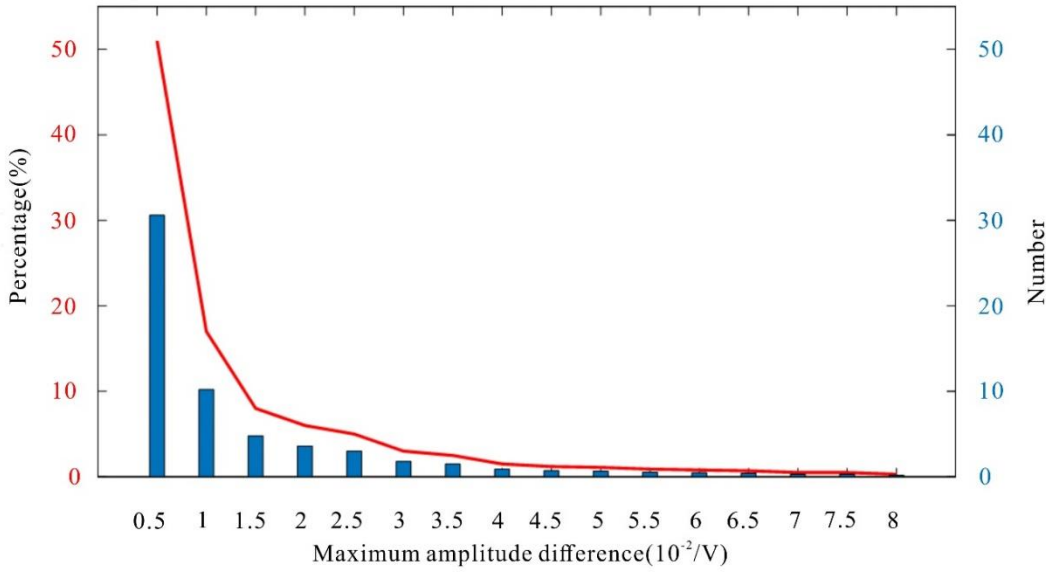

Fig. 13 Denoising result of microseismic noise signal

5. Engineering application

AECNN was applied to denoise microseismic signals HW-Project. Figure 14 shows the results of denoising. In each figure, the first column is real microseismic signal with noise, the second column is denoised signal by AECNN, and the third column is spectrum of the denoising signal. When the pure microseismic signal cannot be restored, the SNR, mean square error (MSE) and correlation coefficient are used as indicators to reflect the effect of signal n denoising, and the SNR distribution after signal denoising is drawn. At the same time, 300 microseismic signals with actual noise were selected for SNR denoising test, 100 of each noise type were selected, and every 5 were in a group, a total of 20 groups of signals.

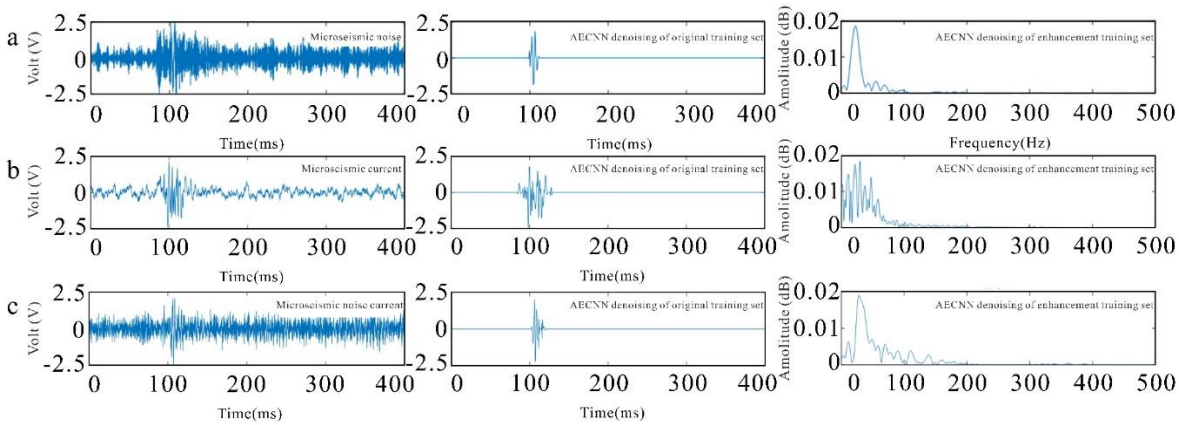

Fig. 14 SNR distribution of AECNN denoising signal.

The AECNN has a well performance for the denoising of the actual monitored signals, as shown in Table 1. In the case of low SNR, microseismic information can still be accurately identified from the noise, and then the noise is removed, the useful information is retained, and the real microseismic signal is restored to the maximum extent. The results of the spectrum diagram indicate that the signal after denoising has main frequency characteristics and clear mode, from which it can be identified as microseismic signal, indicating that the model has a high accuracy in identifying microseismic information, and the SNR of the signal after denoising is significantly improved. The results show that the noise reduction effect of the AECNN is better than the traditional noise reduction method and the noise reduced signal is better for engineering application [34-35].

Tab. 1 Denoising results of noisy microseismic signals

Evaluating indicator	Microseismic signal with different noise		
	MS-CN	MS-CI signal	MS-CN-CI signal
SNR	42.2475	25.2756	37.9705
Mean square error	0.0015	0.0025	0.0204
Correlation coefficient	0.7997	0.9401	0.8326

From the distribution of SNR in Figure 15, it can be seen that the SNR distribution of different types of noised microseismic signals after denoising has obvious distribution intervals. For noised microseismic signals, SNR distribution is mainly (40,50) after denoising; for MS-CI signals, SNR distribution is mainly (20,30) after denoising; for MS-CN-CI signals, SNR distribution is mainly (30,40) after noise denoising. This provides a reference for the denoising of different noised signal types and is beneficial to the classification and recognition of waveform signals.

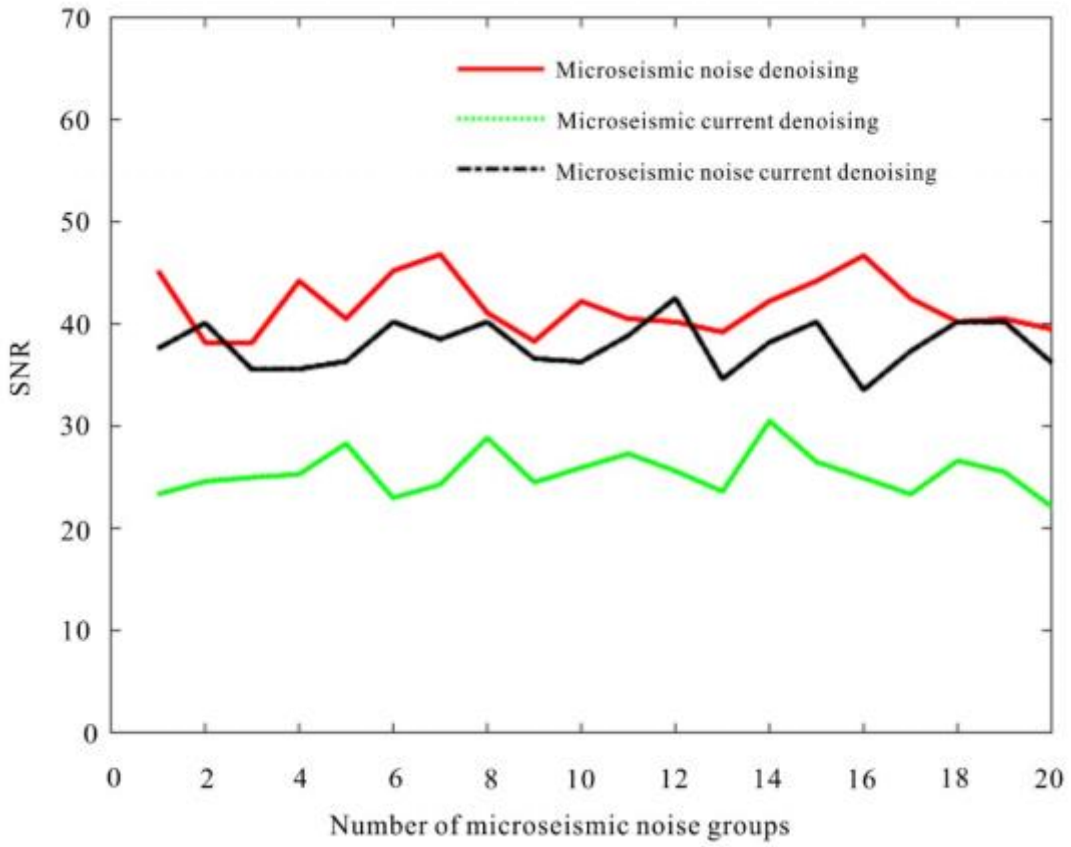

Figure 15 SNR distribution of AECNN denoising signal

6. Conclusion

(1) A denoising model based on convolutional neural network with depth learning called AECNN is proposed. In this model, the features of the input data are learned through a series of convolution pool operations of the automatic encoder, and the input data is reconstructed using the learning features of the decoder to obtain the output data information. Then, a self-coding convolutional neural network based on encoder and decoder is established.

(2) In order to get better training of the mode for insufficient data problem, some data are mirrored and expanded to enhance the dataset. By comparing the results of synthetic signal denoising, it shows the importance of the importance of enhancement of training dataset. The accuracy of the final training set and verification set is 97.7% and 95.2%, while the loss reaches 0.0011 and 0.0016. The model performs well during the training.

(3) The denoising results show that the self-coded convolutional network model has a strong denoising ability for different type of noised microseismic signal, and it can successfully decompose signal with different characteristics into pure microseismic signal and noisy signal.

(4) AECNN shows well performance and for denoising signals for noisy microseismic signal from practical engineering. Under the condition of extremely low SNR, AECNN can accurately identify microseismic information from noise, and then remove noise to get pure microseismic signals. It can be seen that the SNR distribution of different types of noisy microseismic signals after denoising has been significantly improved which is benefit for arrive-time picking and source location.

Acknowledgments: This project was financially supported by the National Natural Science Foundation of China (Grant Nos. 51874065 and U1903112).

Conflict of interest: The authors declare that they have no conflicts of interest.

References:

1. Tang S, Li J, Zhang L, et al. Study on the static critical stress intensity factors of sandstone in a water environment based on semicircular bending specimens. *Theor. Appl. Fract. Mech.*, 2021, 116(103106*)*. doi: 10.1016/j.tafmec.2021.103106

2. Tang S, Li J, Ding S. et al. The influence of water-stress loading sequences on the creep behavior of granite. *Bull Eng Geol Environ* 81, 482 (2022) DOI: 10.1007/s10064-022-02987-3.
3. Ma T, Tang C, Tang L, et al. Mechanism of rock burst forcasting based on micro-seismic monitoring technology. *Chin. J. Rock Mech. Eng.* 2016, 35(3): 470-483. DOI:10.13722/j.cnki.jrme.2014.1083.
4. Li J, Tang S, Li K, et al. Automatic recognition and classification of microseismic waveforms based on computer vision. *Tunn. Undergr. Space Technol.* 2022, 121, 104327. DOI:10.1016/j.tust.2021.104327.
5. Li J, Li K, Tang S. Automatic arrival-time picking of P- and S-waves of microseismic events based on object detection and CNN. *Soil Dyn. Earthq. Eng.* 2022, 164,107560. DOI:10.1016/j.soildyn.2022.107560.
6. Huang N, Wu Z. A review on Hilbert-Huang transform: Method and its applications to geophysical studies. *Rev. Geophys.* 2008, 46(2). DOI:10.1029/2007RG000228.
7. Griffin D, Lim J. Signal estimation from modified short-time Fourier transform. *IEEE Trans. Signal Process.* 1984, 32(2): 236-243. DOI: 10.1109/TASSP.1984.1164317.
8. Arneodo A, Grasseau G, Holschneider M. Wavelet transform of multifractals. *Phys. Rev. Lett.* 1988, 61(20): 2281.DOI: 10.1103/PhysRevLett.61.2281
9. Li C. A tutorial of the wavelet transform. NTUEE, Taiwan, 2010, 21: 22. Available at: http://disp.ee.ntu.edu.tw/tutorial/WaveletTutorial.pdf (Accessed 25 December 2022)
10. Yu D, Cheng J, Yang Y. Application of EMD method and Hilbert spectrum to the fault diagnosis of roller bearings. *Mech Syst Signal Process*. 2005, 19(2): 259-270. DOI: 10.1016/S0888-3270(03)00099-2
11. Boudraa A O, Cexus J C. EMD-based signal filtering. *IEEE Trans Instrum Meas.* 2007, 56(6): 2196-2202. DOI: 10.1109/TIM.2007.907967
12. Jaya Gupta1 Sunil Pathak and Gireesh Kumar. Deep Learning (CNN) and Transfer Learning: A Review. J. Phys Conf Ser, 2273: 012029. DOI: 10.1088/1742-6596/2273/1/012029.
13. LeCun Y, Bengio Y, Hinton G. Deep learning. *Nature*. 2015, 521(7553): 436-444. DOI:10.1038/nature14539.
14. Albawi S, Mohammed T A, Al-Zawi S. 'Understanding of a convolutional neural network. (ICET)', 2017 International Conference on Engineering and Technology (ICET), Antalya, Turkey. 21-23 August 2017. DOI:10.1109/ICEngTechnol.2017.8308186.
15. Gu J, Wang Z, Kuen J, et al. Recent advances in convolutional neural networks. *Pattern Recognit*. 2018, 77: 354-377. DOI: 10.1016/j.patcog.2017.10.013.

16. Li W, Liu H, Wang J. A Deep Learning Method for Denoising Based on a Fast and Flexible Convolutional Neural Network. *IEEE Trans Geosci Remote Sens.* 2021, 60: 1-13. DOI: 10.1109/TGRS.2021.3073001.
17. Guo Yuantao. Research on Denoising Method of Microseismic Signal Based on Convolutional Neural Network. Northeast Pet. Univ. 2021, 0402. DOI: 10.26995/d.cnki.gdqsc.2021.000402.
18. Zhang X, Lin J, Chen Z, et al. An efficient neural-network-based microseismic monitoring platform for hydraulic fracture on an edge computing architecture. *Sensors*. 2018, 18(6): 1828. DOI: 10.3390/s18061828.
19. Zhu W, Mousavi S M, Beroza G C. Seismic signal denoising and decomposition using deep neural networks. *IEEE Trans Geosci Remote Sens.* 2019, 57(11): 9476-9488. DOI:10.1109/TGRS.2019.2926772.
20. Zhao D, Tang C, Li Y. et al. Prediction method of rock burst based on microseismic monitoring and stress field analysis. *Chin. J. Rock Mech. Eng.* (in Chinese), 2005, 24(A01): 4745-4749.
21. Li S. Discussion on Mcroseismic Monitoring Technology and Its Applications to Underground Projects. Chinese J. Undergr. Space Eng., (in Chinese), 2009,5(1): 122-128.
22. Yang L, Zhang B, Ye X. Fast Fourier transform and its applications. *Opto-Electron. Eng*. 2004, 31(S): 1-3.
23. Wang Y, Yao H, Sun X, et al. Representation ability research of AUTO-encoders in deep learning. *Comput. Sci.* 2015, 42(9): 56-60. DOI: 10.11896/j.issn.1002-137X.2015.9.012.
24. Yuan F, Zhang L, Shi J, et al. Theories and Applications of Auto-Encoder Neural Networks: A Literature Survey. *Chin. J. Comput*. 2019, 42(1): 203-230. DOI:10.11897/SP.J.1016.2019.00203.
25. Tang C, Zhu Q, Hong C, et al. Multi-label Feature Selection with Autoencoders and Hypergraph Learning. *Acta Automat. Sin.* 2016, 42(7): 1014-1021. DOI:10.16383/j.aas.2016.c150736.
26. Jiang Z, He Y. Infrared and Visible Image Fusion Method Based on Convolutional Auto-Encoder and Residual Block. *Acta Opt. Sin.* 2019, 39(10): 1015001. DOI: 10.3788/AOS201939.1015001.
27. Jiang J. A study of denoising and interpolation method for reflection seismic data based on Convolutional Auto Encoder. Zhejiang University, 2020. DOI: 10.27461/d.cnki.gzjdx.2020.001374
28. Lin J, Wu X, Chai Y, et al. Structure Optimization of Convolutional Neural Networks: A Survey. *Acta Automat. Sin.* 2020, 46(1): 24-37. DOI: 10.16383/j.aas.c180275.
29. Yang G, Yang J, Li S, et al. Modified CNN algorithm based on Dropout and ADAM optimizer. *J. Huazhong Univ. of Sci & Tech (Natural Science Edition)*, 2018, 46(7): 122-127. DOI:10.13245/j.hust.180723

30. Liu Wanjun, Liang Xunjian, Qu Haicheng. Learning performance of convolutional neural networks with different pooling models. *J. Image Graph*. 2016, 21(9): 1178-1190. DOI: 10.11834/jig.20160907
31. Ji S, Wei S. Building extraction via convolutional neural networks from an open remote sensing building dataset. *Acta Geod. et Cartogr. Sin.* 2019, 48(4): 448-459. DOI: 10.11947/j.AGCS.2019.20180206
32. Yang J, Wang Y. 3D model recognition based on depth convolution neural network. *J. Chongqing Univ. Posts Telecommun. (Natural Science Edition)*. 2019, 31(2): 253-260.
33. Sun X, Mu S, Xu Y, et al. Image recognition of tea leaf diseases based on convolutional neural network. 2018 International Conference on Security, Pattern Analysis, and Cybernetics (SPAC), 14-17 December 2018, Jinan, China. DOI: 10.1109/SPAC46244.2018.8965555.
34. Ding L, Chen Z, Pan Y, et al. Mine microseismic time series data integrated classification based on improved wavelet decomposition and ELM. *Cognit Comput*. 2022, 14, 1526–1546. DOI: 10.1007/s12559-022-09997-z.
35. Lan Z, Gao P, Wang P, et al. Improved wavelet packet noise reduction for microseismic data via fuzzy partition, *IEEE Geosci. Remote Sens. Lett*. 2022, 19, 1-5.DOI: 10.1109/LGRS.2021.3098057